

# Imbalanced Vertices Detection and Applications to Mesh Matching

Jing Yang<sup>1</sup>, Kaiyi Feng<sup>1</sup>, Yongyi Gong<sup>1</sup>, Qi Li<sup>2</sup>, Jianhong Li<sup>1</sup>

<sup>1</sup> Guangdong University of Foreign Studies Cisco School of Informatics Guangzhou, China

<sup>2</sup> Western Kentucky University Department of Computer Science Bowling Green, KY, USA

---

## Abstract

Mesh matching is a helpful application in the field of 3D modeling and geometric processing in which keypoints detection plays an irreplaceable role. In this paper, we present an imbalanced-vertices based method to implement mesh matching which is suitable for the nonuniformly sampled triangulated mesh. The proposed algorithm contains two steps: i) imbalanced vertices detection in 3D meshes, ii) feature description. We utilize a novel cross-angle operator to detect keypoints. Based on the keypoints, we filter out the points that satisfy the imbalanced oriented selection threshold, while describe each with the feature descriptor. Results conclude from the experiments show that our method accomplishes a considerable result compared with the current implementation.

**Index terms** - imbalanced vertices detection, cross-angle, imbalanced oriented selection, mesh matching

---

## 1 Introduction

The study of triangular meshes is the cornerstone of computer graphics and geometric modeling. Different representations of triangular meshes are used for different applications, such as remote sensing, biometric analysis, medical treatment, and intelligent surveillance [4, 3, 8]. Consequently, the representation of mesh feature, geometric information, has been an active research topic including keypoints detection, feature description and so on. However, keypoint detection is the first major phase of a mesh-based application. Current keypoints detection can be classified into two categories [13]: fixed-scale keypoint detection methods and adaptive-scale keypoint detection methods.

Fixed-scale keypoint detection methods define a distinctive point within a predetermined neighborhood, determined by the input scale, as a keypoint. Mohhtarian et al. [9] detected keypoints using the Gaussian and mean curvatures. They declared a point as a keypoint if its curvature value was local maximum. Gal and Cohen-Or [2] introduced saliency grade for keypoint detection, where saliency grade declared the curvature feature around the detected points.

Adaptive-scale keypoint detection methods first build a scale-space for a given range image. The keypoints with extreme distinctiveness measured in both spatial and scale neighborhoods are chosen as keypoints. Darom and Keller [1] utilized density-invariant Gaussian filters to obtain octave meshes, which is robust to varying mesh resolutions. Li and Guskov [6] projected the 3D points onto a series of increasingly smoothed versions of the shape to build up a scale-space.

A critical task in fixed-scale corner detection in 3D meshes is on the distinction of a corner vertex and a vertex with a large curvature which is the fundamental property of a 3D point. Based on curvatures, Sipiran and Bustos [12] generalized Harris detector from 2D images to 3D meshes. Zaharescu et al. [16] introduced the Difference of Gaussian (DOG) operator from 2D image to 3D meshes. The most used curvature in interest point detection is Gaussian curvatures [16, 14, 15]. Moreover, other types of curvatures were also utilized, i.e., normal curvatures [10], mean curvatures [16, 11], overall maximum curvatures [7].

In this paper, we provide Cross Angle Operator to describe local geometric feature and utilize it to detect imbalanced keypoints of a nonuniformly sampled triangulated mesh. The present of experiment study illustrates that our algorithm produces a considerable result.

The rest of the paper is organized as follows: Section 2 introduces the algorithm to detect imbalanced keypoints in 3D meshes. In addition, section 3 describes the implementation of mesh matching and the descriptor we use. Moreover, conclusion is arranged in section 4.

## 2 Imbalanced Vertices in 3D Meshes

In this section, we first propose a vertex geometric feature based operator in terms of the cross angle. Then we introduce imbalance oriented selection to filter out the keypoints. Let  $M$  be a discrete nonuniformly sampled triangulated mesh which can be viewed as a relationship set  $M(V, F)$ , where  $V = \{v_i\}_{1 \leq i \leq P}$  is the set of mesh vertices and  $F_i = \{f_i\}_{1 \leq j \leq Q}$  is the set of faces around a given vertex  $v_i$ .

### 2.1 Cross Angle Operator

Figure 1 illustrates the basic idea of cross angle operator. Let  $T$  be the tangent plane at point  $v$  and  $N_F(\cdot)$  be the operator to get normal vectors of given faces. In order to describe the characteristic of a vertex, we consider the projection of vertex geometric vectors onto its tangent plane  $P_T : a \rightarrow a'$ , where  $a$  are vectors and  $a'$  are the projected vectors on the tangent plane  $T$ . The equation to project vertex-around faces should be written:

$$E_i = P_T(N_F(F_i)) \quad (1)$$

where  $E_i$  is a set of vectors projected on  $T$ . Suppose  $E_i$  is sorted clockwise as its index increases. Then we introduce cross angle operator to measure the relationship between neighbor vectors clockwise:

$$S_i = \arccos \frac{\alpha_j \cdot \alpha_{(j+1) \bmod (|E_i|)}}{\|\alpha_j\| \cdot \|\alpha_{(j+1) \bmod (|E_i|)}\|} \quad (1 \leq j \leq |E_i|) \quad (2)$$

where  $S_i$  is the cross angle set,  $\alpha$  represents the vector in  $E_i$ ,  $(\cdot) \bmod (\cdot)$  is modulo operation,  $|\cdot|$  is the cardinality of a given set, and  $\|\cdot\|$  is the Euclidean norm operator.

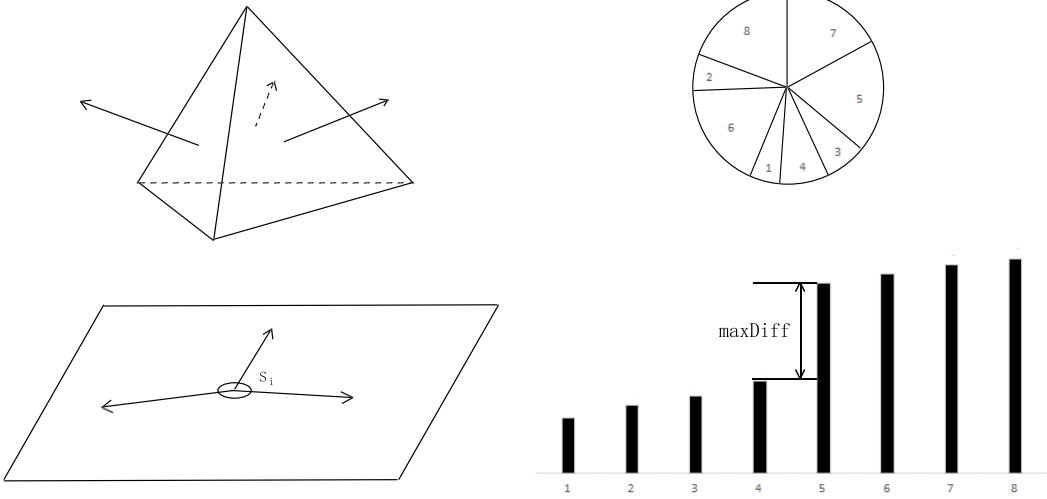


**Figure 1:** The basic idea of the cross angle operator. Project all the normal vectors around a given vertex onto its tangent plane and construct an ordered angle set.

**Figure 2:** Illustration of the imbalance oriented selection. Eight bars are sorted in term of their values, which determine a balanced vertex in this case, where the index of maximum difference is 2 ( $\neq$  half of 8 directions)

## 2.2 Imbalance Oriented Selection

Imbalanced point detection in 2D images aims to minimize the occurrences of edge points [5]. Denote  $I$  a gray value image,  $p$  a local point,  $\theta_i = (i-1) \cdot \frac{2\pi}{N}$ , and  $l_i = (\cos \theta_i, \sin \theta_i)$  for  $i = 1, 2, \dots, N$ . Denote  $\frac{\partial I}{\partial l_i}(p)$  a directional derivative of  $p$  along  $l_i$  direction. We cluster  $\left\{ \frac{\partial I}{\partial l_i}(p) \right\}_{i=1}^N$  into two classes in terms of their magnitudes  $\left| \frac{\partial I}{\partial l_i}(p) \right|$ . If two clusters have the same size, the image point  $p$  is balanced.

The sorting method proposed in [5] to classify  $\left\{ \frac{\partial I}{\partial l_i}(p) \right\}_{i=1}^N$  can be generalized to extract 3D imbalanced vertices with the favor of cross angle operator. Let  $maxDiff$  be the max difference and  $D$  be the index of maximum difference:

$$maxDiff = \max_j (\beta_{j+1} - \beta_j) \quad (1 \leq j \leq N-1) \quad (3)$$

$$D = \arg \max_j (\beta_{j+1} - \beta_j) \quad (1 \leq j \leq N-1) \quad (4)$$

where  $\beta$  represents vector in  $S_i$ . Given a threshold on homogeneity  $T_h$ , the imbalanced vertex can be defined under the condition that  $maxDiff < T_h$ :

$$IMB(v_i) = \begin{cases} 1 & D_i < \frac{N}{2} \\ 0 & \text{else} \end{cases} \quad (5)$$

## 3 Experiment

In this section, we present a visual presentation of our across angle operator based imbalanced vertex detection with a comparison of current detection methods. Furthermore, we introduce the application of imbalanced vertices on mesh matching utilizing feature descriptor to demonstrate the efficiency of imbalanced keypoints.

### 3.1 Visual Comparison

Figure 3 and figure 4 present results on different datasets utilizing different detection methods: normal vector based detection, mean curvature based detection, and cross angle based detection. As the results illustrate, the cross angle based detection generates feature based results. Moreover, results obtained by mean feature based detection seem to be an informative method but emphasizing the characteristic of the given model. However, normal vector based detection is the worst performer.

### 3.2 Mesh Matching

To implement mesh matching, we adapt the descriptor [17] for each mesh. The descriptor  $t_v$  for vertex  $v$  is computed within a support region. After the definition of the domain, a local coordination system is built up to maintain its rotation invariance. Then, a histogram of gradient is computed to analyse statistic properties of each imbalanced keypoints. As a result, descriptors of each mesh match in terms of the Euclidean distance.

**Support Region.** The radius of circular support region  $r$  is chosen adaptively based on a global measure:

$$r = \left[ \sqrt{\frac{\alpha_r A_M}{\Pi}} \right] \quad (6)$$

where  $\alpha_r \in (0, 1)$  is the proportion factor,  $A_M$  denotes the total area of mesh  $M$  and  $[ \cdot ]$  rounds the results. In practice, we use  $r$  corresponding to  $\alpha_r = 0.01$ .

**Local Coordinate System.** A local coordinate system can be built using the unit vector  $n_i$  orthogonal to the tangent plane  $T_i$  at vertex  $v_i$  and a pair of orthogonal vectors residing in  $T_i$ . Given a vector  $\alpha_r \in T_i$ , a local coordinate system is constructed as

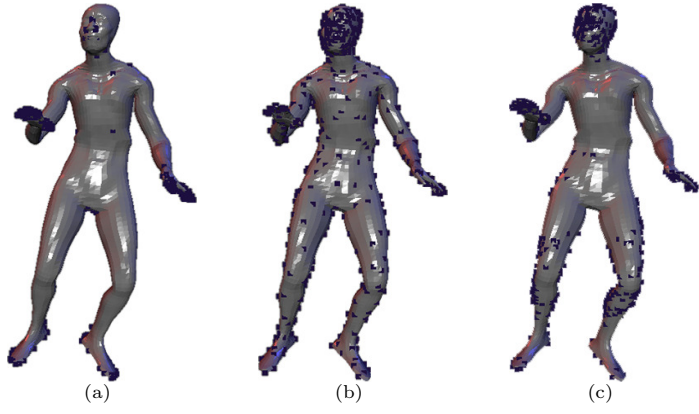


**Figure 3:** Visual comparison of different feature based keypoints detection: (a) Normal vector based detection; (b) Mean curvature based detection; (c) Cross angle based detection

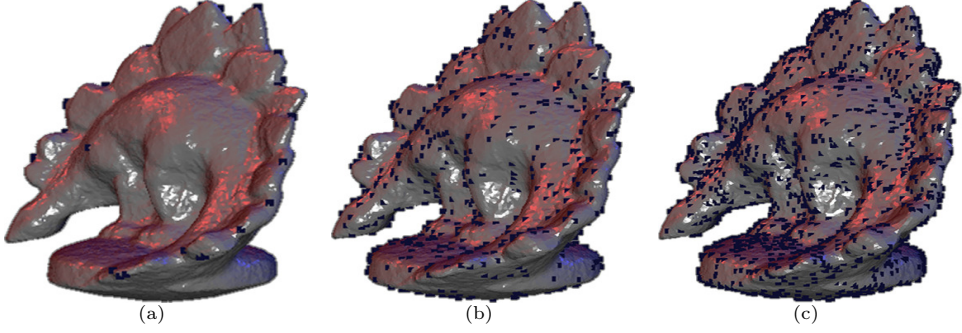


**Figure 4:** Visual comparison of different feature based keypoints detection: (a) Normal vector based detection; (b) Mean curvature based detection; (c) Cross angle based detection

$\{a_i, n_i, a_i \times n_i\}$ . Vector  $a_i$  is computed as the direction associated to the dominant bin in a polar histogram, with  $b_a = 36$  bins. The histogram is constructed by the projection of participating neighboring vertices on  $T_i$  and taking into account their gradient magnitudes which is weighted by a Gaussian with  $\sigma = r/2$ .

**Histogram Descriptor.** Local coordinate system spans three orthonormal planes. For each of the three planes, a 2-level histogram is computed. To mention first, the plane is divided in  $b_s = 4$  polar slices, starting with an origin and continuing in the direction dictated by the right-hand rule, with respect to the other orthonormal vector. When projected onto the plane, the participating neighboring vertices  $v_j$  will fall within one of the spatial slices. Besides, for each spatial slice, the space is divided into  $b_o = 8$  orientation slices. The projected gradient vector  $\nabla_M f(v_i)$  of the vertices projected onto spatial slice are used to determine the orientation slice. The final descriptor is obtained by concatenating the  $b_s \cdot b_o$  histogram values for each of the three orthonormal planes.

**Mesh Matching.** We validate the proposed imbalanced keypoints detection and descriptor on mesh matching approach. Let  $M_1$  and  $M_2$  denote two different meshes of the same object with unnecessarily equal number of vertices. Using the proposed detection method,  $n_1$  imbalanced keypoints are detected on  $M_1$  characterized by descriptors  $d_i^1, i \in [1, n_1]$ , while  $n_2$  imbalanced keypoints are detected on  $M_2$  characterized by descriptors  $d_j^2, j \in [1, n_2]$ . For each descriptor  $d_i^1$  from mesh  $M_1$ , the proposed algorithm find the best matching descriptor  $d_j^2$  from mesh  $M_2$  in terms of the Euclidean distance  $d_{ij} = \|d_i^1 - d_j^2\|$  which is an intuitive greedy algorithm. The matching results generated demonstrate that imbalanced points on  $M_1$  matching corresponding points on  $M_2$ .

## 4 Conclusion

In this paper, we boost the basic idea of imbalanced pixels in 2D images to 3D meshes for imbalanced keypoint detection. Cross angle operator describes the attribute of each vertices, and imbalance oriented selection seeks suspected vertices. Moreover, based on the vertices we found, we combine them with descriptors to implement mesh matching. The experimental results show that detected points on each mesh matches well.

## References

- [1] T. Darom and Y. Keller. Scale-invariant features for 3-d mesh models. *Pattern Analysis and Machine Intelligence IEEE Transactions on*, 21(5):2758–2769, 2012.
- [2] R. Gal and D. Cohen-Or. Salient geometric features for partial shape matching and similarity. *Acm Transactions on Graphics*, 25(1):130–150, 2006.
- [3] Y. Guo, J. Wan, M. Lu, and W. Niu. A parts-based method for articulated target recognition in laser radar data. *Optik*, 124(17):2727–2733, 2012.
- [4] Y. Lei, M. Bennamoun, M. Hayat, and Y. Guo. An efficient 3d face recognition approach using local geometrical signatures. *Pattern Recognition*, 42(2):509–524, 2014.

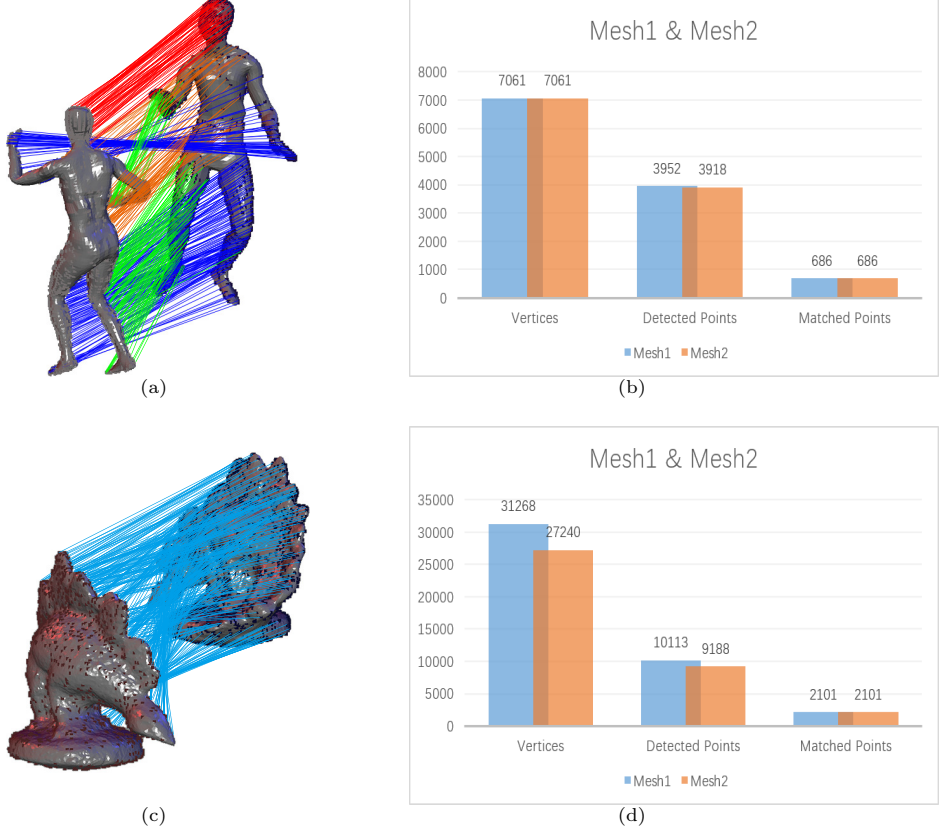


**Figure 5:** (a)(c)Visualization of matching results; (b)(d) Data analysis

- [5] Q. Li, J. Ye, and C. Kambhamettu. Interest point detection using imbalance oriented selection. *Pattern Recognition*, 42(2):672–688, 2008.
- [6] X. Li and I. Guskov. Multiscale features for approximate alignment of point-based surfaces. *Eurographics Symposium on Geometry Processing*, pages 217–226, 2005.
- [7] F. Liu, D. Zhang, and L. Shen. Study on novel curvature features for 3d fingerprint recognition. *Neurocomputing*, 168:599–608, 2015.
- [8] A. Mian, M. Bennamoun, and R. Owens. On the repeatability and quality of keypoints for local feature-based 3d object retrieval from cluttered scenes. *International Journal of Computer Vision*, 89(2):348–361, 2010.
- [9] F. Mokhtarian, N. Khalili, and P. Yuen. Multi-scale free-form 3d object recognition using 3d models. *Image and Vision Computing*, 19(5):271–281, 2001.
- [10] J. Novatnack and K. Nishino. Scale-dependent/invariant local 3d shape descriptors for fully automatic registration of multiple sets of range images. *European Conference on Computer Vision-eccv*, pages 440–453, 2008.
- [11] M. Schlattmann, P. Degener, and R. Klein. Scale space based feature point detection on surfaces. *Journal of Wscg*, 16:1–3, 2008.
- [12] I. Sipiran and B. Bustos. Harris 3d: a robust extension of the harris operator for interest point detection on 3d meshes. *The Visual Computer*, 27(11):963–976, 2011.
- [13] F. Sohel, J. Wan, M. Lu, and M. Bennamoun. 3d object recognition in cluttered scenes with local surface features: A survey. *Pattern Analysis and Machine Intelligence IEEE Transactions on*, 36(11):2270–2287, 2014.
- [14] J. Sun, M. Ovsjanikov, and L. Guibas. A concise and provably informative multi-scale signature based on heat diffusion. *Pattern Analysis and Machine Intelligence IEEE Transactions on*, 28(5):1383–1392, 2009.
- [15] G. Tam, Z. Cheng, Y. Lai, F. Langbein, Y. Liu, A. Marshall, R. Martin, X. Sun, and P. Rosin. Registration of 3d point clouds and meshes: A survey from rigid to nonrigid. *IEEE Transactions on Visualization and Computer Graphics*, 19(7):1199–1217, 2013.
- [16] A. Zaharescu, E. Boyer, and R. Horaud. Keypoints and local descriptors of scalar functions on 2d manifolds. *International Journal of Computer Vision*, 100(1):78–98, 2012.
- [17] A. Zaharescu, E. Boyer, K. Varanasi, and R. Horaud. Surface feature detection and description with applications to mesh matching. *Proceedings of IEEE Conference on Computer Vision and Pattern Recognition*, pages 373–380, 2009.